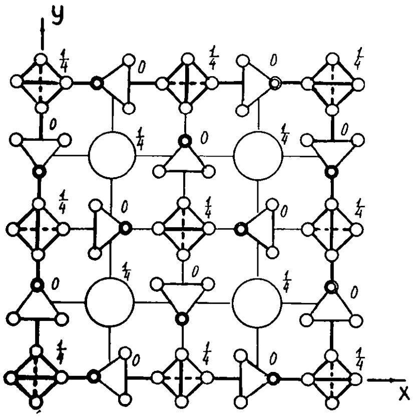

Fig. 2. Orientational structure of the cubic 32-molecule intermediate phase of deuteromethane (space group *Fm*3*c*). The projection is of two layers on the plane (001).

Tetragonal lattice distortion along *z* resulting from the transition of the cubic intermediate phase into the low-temperature phase seems to be due to a preferred molecular orientation in planes parallel to the *c* axis and containing molecules with point symmetry C_1.

Thus, in the low-temperature phase of deuteromethane, molecules reside at three types of sites which essentially differ in their lattice-field symmetry; however, contrary to the results of Maki, Kataoka & Yamamoto (1978), our experiments provide evidence for lower point symmetry. It should be noted that some recent work (Medina & Daniels, 1978; Kobashi, 1978) on Raman and IR spectra in the intermediate and low-temperature phases of methane under pressure at 4·2 K also revealed three types of molecular point symmetries in α-CH_4 which have very different molecular fields.

The authors thank I. N. Krupskii and A. I. Erenburg for discussion of the results.

References

Arzi, G. & Sandor, G. (1975). *Acta Cryst.* **A31**, S188.

Baer, D. R., Fraase, B. A., Riehl, D. H. & Simmons, R.D. (1978). *J. Chem. Phys.* **68**(4), 1411–1417.

International Tables for X-ray Crystallography (1952). Vol. I. Birmingham: Kynoch Press.

James, H. M. & Keenan, T. A. (1959). *J. Chem. Phys.* **31**(1), 12–41.

Kitaigorodskii, A. I. (1971). *Molecular Crystals.* Moscow: Nauka.

Kobashi, K. (1978). Abstracts. Symposium on Solid Methane. McMaster Univ., Hamilton, Canada, October 13–14.

Krasnov, K. S., Timoshin, V. S., Danilova, T. G. & Khandozhko, S. V. (1968). *Molekulyarnye Postoyannye Neorganicheskikh Soyedineniy*, p. 158. Leningrad: Khimiya.

Maki, K., Kataoka, Y. & Yamamoto, T. (1978). *Theory of Phase Transitions in Solid Methanes.* XII. Preprint, Kyoto Univ., Japan.

Medina, F. D. & Daniels, W. B. (1978). Abstracts. Symposium on Solid Methane. McMaster Univ., Hamilton, Canada, October 13–14.

Press, W. (1972). *J. Chem. Phys.* **56**(6), 2597–2609.

Press, W. & Hüller, A. (1974). *Anharmonic Lattices, Structural Transitions and Melting*, p. 185. Noordhoff: Riste.

Prokhvatilov, A. I., Gasan, V. M. & Erenburg, A. I. (1970). *Fiz. Kondens. Sostoyaniya*, **10**, 135–153.

Titov, Yu. G., Verkhorobin, L. F. & Matyushenko, N. N. (1972). *Kristallografiya*, **17**(5), 1053–1059.

Acta Cryst. (1980). B**36**, 1580–1588

The Structures of Two Forms of Tetraphenyldithiapyranylidene* Polyiodide, One-Dimensional Organic Conductors

By Henry R. Luss and Douglas L. Smith

Research Laboratories, Eastman Kodak Company, Rochester, New York 14650, *USA*

(*Received* 14 *September* 1979; *accepted* 11 *February* 1980)

Abstract

The crystal structures of two forms of the ion–radical salt of tetraphenyldithiapyranylidene (φ_4DTP) and iodine have been determined from X-ray diffractometer data. Both structures were solved by Patterson and Fourier methods and refined by full-matrix least squares. One form (DTPI1) is orthorhombic, *Fddd*, with $a = 30{\cdot}99$ (3), $b = 54{\cdot}83$ (7), $c = 3{\cdot}700$ (4) Å and $Z = 8$. The second form (DTPI2) is tetragonal, $P\bar{4}b2$, with $a = 19{\cdot}74$ (2), $c = 3{\cdot}721$ (5) Å and $Z = 2$. In addition to the Bragg reflections, diffuse streaks on precession photographs indicate disordered lattices incommensurate along *c* with a repeat of $c' = 9{\cdot}39$ Å

---

* 3,3′,5,5′-Tetraphenyl-4,4′-dithia-1,1′-bi-2,5-cyclohexadienylidene.

0567-7408/80/071580-09$01.00

for DTPI1 and 9·7 Å for DTPI2. In both compounds, the φ_4DTP donor molecules are not planar but have crystallographic 222 symmetry and stack uniformly along c. In DTPI1 the I atoms are present as both I_3^- and I_5^- ions which occupy channels parallel to the donor stacks. A model with one chain of I_3^- ions and two chains of I_5^- ions per donor stack refined to $R = 0{\cdot}057$. Only I_3^- ions are present in DTPI2 and there are two chains of these ions per stack of donor molecules. A model in which 50% of the I_3^- ions were incommensurate with the φ_4DTP lattice refined to $R = 0{\cdot}042$. There are no significant differences in the φ_4DTP bond lengths between the two forms, indicating that the formal charge on the donor molecules is about the same in both forms, consistent with the stoichiometries $\varphi_4\mathrm{DTP}(I_3)_{0\cdot36}(I_5)_{0\cdot40}$ for DTPI1 and $\varphi_4\mathrm{DTP}(I_3)_{0\cdot72}$ for DTPI2.

Introduction

The structures and physical properties of highly conducting organic charge-transfer salts have been extensively investigated in recent years (Perlstein, 1977; Stucky, Schultz & Williams, 1977). These materials are characterized by the presence of segregated stacks of donor and acceptor molecules and a mixed-valence state. The most efficient organic conductors contain molecules which upon one-electron oxidation or reduction form a new aromatic sextet whose aromaticity can migrate by mixed-valence interaction (Perlstein, 1977). Such is the case with the donor molecule, φ_4DTP:

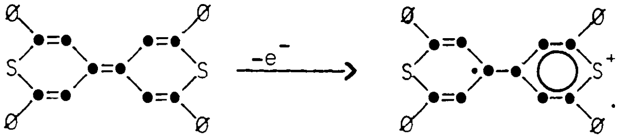

The ion–radical salt φ_4DTP:TCNQ and its oxygen analog φ_4DP:TCNQ have been examined and single-crystal conductivities at room temperature of 15 000–25 000 and 4000 Ω^{-1} m^{-1}, respectively, were reported (Alizon *et al.*, 1977; Isett, Reynolds, Schneider & Perlstein, 1979*a*). It is not known, however, to what extent charge transport along the φ_4DTP stack contributes to the conductivity in these materials, and so complexes without TCNQ have been sought.

Previously, Isett & Perez-Albuerne (1977) and Isett (1978) had prepared and studied an ion–radical salt of tetrathiotetracene (TTT) with stoichiometry $\mathrm{TTT_2I_3}$. A single-crystal conductivity of 10^5 Ω^{-1} m^{-1} at room temperature along the stacking axis was reported. The crystal structure (Smith & Luss, 1977) showed that this material fits the criteria described above for an efficient organic conductor. Subsequently, two crystal forms of the ion–radical salt of φ_4DTP and iodine were prepared and studied by Isett, Reynolds, Schneider & Perlstein (1979*b*). One form (DTPI1) is orthorhombic with a single-crystal conductivity of 200 Ω^{-1} m^{-1} at room temperature. The other form (DTPI2) is tetragonal and has a single-crystal conductivity at room temperature of 12 000 Ω^{-1} m^{-1}. We report here the crystal structures of these two materials.

Experimental

Blue-gray, long, six-sided, prismatic (c) crystals of DTPI1 were grown at the interface between a toluene solution of φ_4DTP and an acetonitrile solution of I_2 at 328 K. The ratio of φ_4DTP/I_2 was 1/1·15. Greenish-gray, long, square, prismatic (c) crystals of DTPI2 were grown by slow evaporation of THF/acetonitrile solutions mixed in the ratio of 1/1·6 for φ_4DTP/I_2. This procedure gave both forms, with the orthorhombic form predominant.

Crystal data for both forms are given in Table 1. The stoichiometries given were those used in the final refinements. The lattice constants were refined by least-squares analysis of the setting angles of 11 reflections (27° < 2θ < 45°) for DTPI1 and 10 reflections (29° < 2θ < 34°) for DTPI2, centered through narrow slits at low source angle on a Picker diffractometer.

Systematic absences were determined from precession photographs which also showed, for both compounds, a pattern of diffuse density perpendicular to the short (c) axis with a period incommensurate with c. Diffuse streaks due to one-dimensionally disordered polyiodide chains and having a supercell repeat distance incommensurate with the organic subcell have often been reported, *e.g.* $\mathrm{TTT_2I_3}$ (Smith & Luss, 1977) and 5,10-diethyl-5,10-dihydrophenazinium iodide (Endres *et al.*, 1979). These compounds are type (d) in the classification given by Herbstein & Kapon (1972).

Table 1. *Crystal data*

	DTPI1	DTPI2
Formula	$C_{34}H_{24}I_{3\cdot09}S_2$	$C_{34}H_{24}I_{2\cdot15}S_2$
M_r	889	770
Crystal system	Orthorhombic	Tetragonal
Space group	*Fddd*	$P\bar{4}b2$
Unit cell a	30·99 (3) Å	19·74 (2) Å
b	54·83 (7)	
c	3·700 (4)	3·721 (5)
V	6287 (12) Å^3	1450 (3) Å^3
Z	8	2
D_c	1·88 Mg m^{-3}	1·76 Mg m^{-3}
D_m	1·92	1·79
$F(000)$	3390	748
μ(Mo $K\alpha$)	3·3 mm^{-1}	2·5 mm^{-1}

Only one weak diffuse streak was visible on the *h*0*l* and 0*kl* photographs of DTPI1, which corresponded to a spacing of about 3·13 Å. By analogy to TTT_2I_3, which had several additional weak streaks, this may be the third order of a supercell repeat of 9·39 Å. However, it could also be the fifth order of a supercell repeat of 15·65 Å characteristic of I_5^- (Herbstein & Kapon, 1972). The diffuse scattering for DTPI2 is more complex. In addition to a strong third-order streak, there are five weak streaks corresponding to orders 1, 2, 4, 6 and 7 of a 9·7 Å period. The intensity pattern is similar to that observed in other polyiodide complexes (see, *e.g.*, Smith & Luss, 1977; Huml, 1967; Endres *et al.*, 1976, 1979). In addition, there is a weak streak at a spacing of 2·7 Å which corresponds to 9·7 Å if measured from the $l = 1$ row of spots.

For DTPI1, systematic absences (hkl: $h + k$ and $k + l \neq 2n$, $0kl$: $k + l \neq 4n$, $h0l$: $h + l \neq 4n$, $hk0$: $h + k \neq 4n$) established the space group as *Fddd*. For DTPI2, systematic absences ($0kl$: $k \neq 2n$ and $h00$: $h \neq 2n$) were consistent with space groups *P*4*bm*, $P\bar{4}b2$ and *P*4/*mbm*. $P\bar{4}b2$ was chosen from crystal-packing considerations and confirmed by successful structure refinement.

A DTPI1 crystal 0·08 × 0·10 × 0·76 mm was used for intensity-data collection on a card-controlled Picker four-circle diffractometer at 297 ± 2 K with Zr-filtered Mo radiation. 1414 unique reflections for $2\theta < 50°$ were measured by the θ–2θ scan method at a 2θ scan rate of 1° $\min^{-1}$. Scans were from 0·95° below the $K\alpha_1$ peak to 0·70° above the $K\alpha_2$ peak, except for low-angle reflections where the lower limit was adjusted to avoid the $K\beta$ peak. Backgrounds were measured for 20 s at each end of the scan. A standard reflection (11,19,1), remeasured every fiftieth reflection, was used to scale the data. The standard showed fluctuations of as much as ±18% from the mean; these fluctuations correlated with laboratory conditions, especially temperature and utility load, and were not caused by crystal instability.

For DTPI2, a crystal 0·15 × 0·20 × 0·76 mm was used for data collection; 1021 unique reflections for $2\theta \leq 55°$ were measured under similar conditions except that the scan range was broadened to 1·2° below $K\alpha_1$ to 0·8° above $K\alpha_2$. Intensities of the standard reflection (10,2,1) varied ±3% over the data-collection period and were used to correct the data.

The intensities were reduced to structure amplitudes after correction for background, Lorentz and polarization effects. Absorption corrections were not applied; we estimate the maximum error in I caused by absorption to be ±5% in DTPI1 and ±10% in DTPI2. Standard deviations, $\sigma(I)$, were based on counting statistics and corrected to $\sigma(F)$. 1024 reflections for DTPI1 and 864 reflections for DTPI2 had $I > \sigma(I)$ and were considered observed. Unobserved reflections were not included in the refinement.

Structure determination and refinement

Both structures were solved by the heavy-atom method from *c*-axis ($E^2 - 1$) Patterson projections and subsequent three-dimensional electron density maps. Refinement was by full-matrix least squares (Busing, Martin & Levy, 1962), and included an extinction correction for DTPI2 (Luss & Smith, 1973; Larson, 1969). Weights were defined as $|\sigma^2(F_o) + (0{\cdot}03F_o)^2|^{-1}$ and the atomic scattering factors were taken from *International Tables for X-ray Crystallography* (1974). The agreement factors are $R = \sum||F_o| - K|F_c||/\sum F_o$, $R_w = |\sum w(|F_o| - K|F_c|)^2/\sum wF_o^2|^{1/2}$.

*DTPI*1

The unit-cell data gave much initial information about the structure. Space-group restrictions require the donor molecule to have crystallographic 222 symmetry. The short *c* axis dictated stacking in this direction so only the orientation (S···S axis along *a* or *b*) and twists of the φ_4DTP moiety and the locations of the I atoms were unknown. From the streaking on the precession photographs it was presumed that the I atoms form polyiodide ions which lie in columns along *c* with the stoichiometry requiring three of these chains per stack of donor molecules. One-dimensional disorder arises because adjacent iodine columns can be shifted somewhat arbitarily relative to one another and also because of the incommensurability of the lattices.

Because of the disorder of the I atoms, a three-dimensional Patterson map contained columns of density along *c* and did not unambiguously yield atomic parameters. An *hk*0 Patterson projection more clearly revealed the *x*,*y* positions of all the atoms including the I channels, and a subsequent three-dimensional electron density map phased with S and C(1) revealed the *z* parameters for the remaining donor-molecule atoms. A model was also obtained for

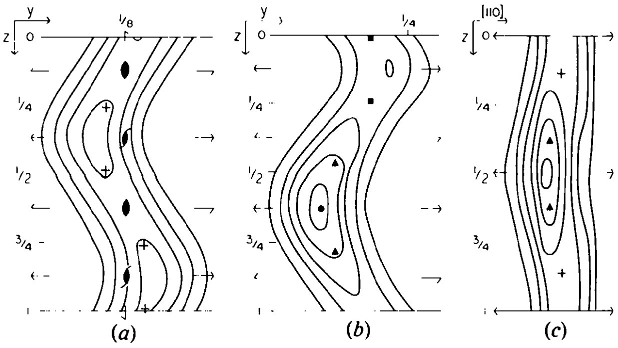

Fig. 1. Electron density distributions in the iodine channels. Contours are at intervals of 5 e Å ^{3} starting at 5 e Å^{-3}. (*a*) I(1) channel of DTPI1 at $x = \frac{3}{8}$. I(1) positions are indicated by +. (*b*) I(2),I(3) channel in DTPI1 at $x = \frac{1}{8}$. ● I(2*A*), ▲ = I(2), ■ = I(3). (*c*) I(1), I(2) channel in DTPI2 plotted for a diagonal section. + = I(1), ▲ = I(2).

the I atoms. Following refinement with anisotropic temperature factors, a difference electron density map revealed the H atom positions.

Refinement was hampered by the disordered I atoms. Although the streaking on the precession photographs indicated an iodine lattice which was incommensurate with the donor lattice, it soon became obvious that the major portion of the I atoms lay on the donor lattice. The I atoms made substantial contributions to structure factors with $l \neq 0$, and the electron density in the iodine channels was not uniform but varied along both *b* and *c*. Electron density sections though the two unique iodine channels, calculated using the final atomic positions for I indicated, are shown in Fig. 1(*a*) and (*b*). The third channel per donor stack is generated from the channel in Fig. 1(*b*) by the cell symmetry shown.

The observed density of the crystals implies a unit-cell composition of eight φ_4DTP(I)$_{3\cdot2}$ units which in *Fddd* corresponds to 0·8 I atoms per asymmetric unit. Many models of disordered I atoms with fractional occupancy factors were tested. Initially we used models with chains of I_3^- ions in all channels and obtained an *R* as low as 0·058 ($R_w = 0\cdot068$). During the refinement, resonance Raman spectra (Trotter, 1979) indicated the presence of both I_3^- and I_5^- but not I_2. The relative amounts of I_3^- and I_5^- were not established by the Raman study, but a model in which there was one channel of I_3^- and two channels of I_5^- refined to $R = 0\cdot057$ ($R_w = 0\cdot068$). Although the I_3^- and the $\mathrm{I}_3^-/\mathrm{I}_5^-$ refinements did not yield significantly different agreement factors, we believe the $\mathrm{I}_3^-/\mathrm{I}_5^-$ model is the more reasonable one. A few of the models will now be discussed in more detail. Each refinement mentioned utilized isotropic thermal parameters for H and anisotropic thermal parameters for all other atoms. It should be noted that for disorders of this type, the coordinates chosen for the partially occupied disordered sites actually represent a mean value for a range of unresolved, closely spaced, atomic positions. This is usually indicated by a large value for the anisotropic thermal parameter β_{33} for which the present structures are no exception.

The unique channel at $x,y = \frac{3}{8},\frac{1}{8}$ (Fig. 1*a*) contains two equivalent electron density maxima separated by $c/2$. The peaks lie at different *y* values on twofold axes along *b* and are related by a twofold screw axis along *c*. We have considered the peaks to be caused by the overlap of partially occupied, disordered atomic sites situated between the twofold axes, *i.e.* I(1) sites approximately $c/4$ apart. Then the chain can be composed of an infinite sequence of I_3^- units occupying 2·5 or 2·75 cells, depending on the non-bonded distance adopted, with bonding between atoms about $3c/4$ apart:

$$\mathrm{I}\underset{2\cdot8\ \text{Å}}{\overset{3c/4}{\rule{2em}{0.4pt}}}\mathrm{I}\underset{2\cdot8\ \text{Å}}{\overset{3c/4}{\rule{2em}{0.4pt}}}\mathrm{I}\underset{3\cdot7\ \text{or}\ 4\cdot6\ \text{Å}}{\overset{c\ \text{or}\ 5c/4}{\cdots\cdots\cdots}}\mathrm{I}.$$

The shorter non-bonding distance yields 0·3 for the site-occupancy factor and the longer, 0·273. The I_3^- ions are not linear but are bent by about 10°, probably because of close contacts with the donor H atoms. These contacts also act to inhibit the formation of the incommensurate lattice whose dimension, 9·39 Å, might be considered the natural repeat distance of longitudinally unconstrained I_3^- units in this crystal. Thus the 2·5 cell repeat (9·25 Å), being shorter than this, is unlikely, leaving the 2·75 cell repeat (10·18 Å) as the more probable.

The channel at approximately $x,y = \frac{1}{8},\frac{1}{4}$ (Fig. 1*a*) represents one of the other two equivalent iodine columns associated with a donor stack. It resembles the previous case in that there are two distinct electron density maxima separated by $c/2$ which lie at different *y* values on twofold axes along *b*. The situation differs, however, because the maxima are not symmetry related and have different densities in the ratio of 2/1, indicating that the positions are unequally occupied. As before, the peaks can be considered to arise from the overlap of partially occupied, disordered atomic sites situated between the twofold axes with approximate location of I(2) at $c/2$ and $3c/4$ and I(3) at $c/4$ and $z = 0$.

Chains of I_3^- with I(2) and I(3) arranged as in the I(1) channel are not reasonable because such an arrangement should give equal electron densities and the occupancies would total $3 \times 0\cdot273 = 0\cdot819$, which overestimates the iodine content of the crystal. Refinement of such a model, but with equal occupancies adjusted to 0·265 to satisfy stoichiometry, converged to $R = 0\cdot067$ ($R_w = 0\cdot092$).

Unequal occupancies were also assigned to the iodine atoms. In the extreme case of I(2)/I(3) = 2/1, the I_3^- ions would occupy three unit cells:

$$\mathrm{I}(2)\underset{2\cdot8\ \text{Å}}{\overset{3c/4}{\rule{2em}{0.4pt}}}\mathrm{I}(2)\underset{2\cdot8\ \text{Å}}{\overset{3c/4}{\rule{2em}{0.4pt}}}\mathrm{I}(3)\underset{5\cdot6\ \text{Å}}{\overset{3c/2}{\cdots\cdots}}\mathrm{I}(2).$$

The occupancies would be 0·333 for I(2) and 0·167 for I(3). A model with these occupancies and an occupancy of 0·3 for I(1) refined to $R = 0\cdot068$ ($R_w = 0\cdot091$). To find the occupancy parameters which would give the best fit to the data, we refined the occupancy parameters of I(1), I(2) and I(3) using only *hkl*, $l \neq 0$ data to eliminate any contribution of iodine to the incommensurate lattice. Because of high correlations, the β_{33} parameters for the I atoms were held constant at 0·18. Occupancies of 0·28, 0·30 and 0·21 for I(1), I(2) and I(3), respectively, resulted. Refinement of all atoms with these occupancies and the complete data set converged to $R = 0\cdot058$ ($R_w = 0\cdot068$). The occupancy for I(1) and the total occupancy (0·79) were both encouragingly close to expected values. The problem with the I(2) and I(3) occupancies is that they require variable non-bonded intervals between I_3^- units in the chain, either $5c/4$ or $6c/4$.

At this time we became aware of the probable presence of both I_3^- and I_5^- in the crystal. Consideration of bond lengths in the donor molecule (discussed later) suggested the possibility that I_5^- ions occupied the two symmetry-related I(2)/I(3) channels and I_3^- ions occupied the I(1) channel. An approximately linear I_5^- molecule can be formulated if one postulates an additional I atom [I(2*A*)] at $z = \frac{5}{8}$ on the twofold axes:

$$\mathrm{I}(3)\underset{2\cdot8\,\text{Å}}{\overset{3c/4}{\rule{2.5em}{0.4pt}}}\mathrm{I}(2)\underset{3\cdot2\,\text{Å}}{\overset{7c/8}{\rule{2.5em}{0.4pt}}}\mathrm{I}(2A)\underset{3\cdot2\,\text{Å}}{\overset{7c/8}{\rule{2.5em}{0.4pt}}}\mathrm{I}(2)\underset{2\cdot8\,\text{Å}}{\overset{3c/4}{\rule{2.5em}{0.4pt}}}\mathrm{I}(3)\underset{6\cdot5\,\text{Å}}{\overset{7c/4}{\cdots\cdots}}\mathrm{I}(3).$$

These distances agree with those reported by Herbstein & Kapon (1972) for I_5^- in a similar complex. The occupancies relative to the asymmetric unit are 0·2 for I(2) and I(3) and 0·1 for I(2*A*), which combine with 0·273 for I(1) to give a total occupancy of 0·773. The addition of atom I(2*A*) is consistent with the higher electron density around I(2) compared to I(3). Refinement with these occupancies gave $R = 0{\cdot}057$ ($R_w = 0{\cdot}068$). Although there is no significant improvement in agreement compared to the best I_3^- model, the I_5^-/I_3^- model appears to be more chemically reasonable and we have taken it as our refined structure.

On the final cycle, only six out of 139 parameter shifts were $>0{\cdot}1\sigma$ with a maximum shift of $0{\cdot}27\sigma$. A difference electron density map contained residual density within $\pm0{\cdot}37$ e Å^{-3}. The residual density in the I channels was positive but $\leq0{\cdot}22$ e Å^{-3}, indicating that the I atom contributions may have been slightly underestimated. The final atomic parameters, with estimated standard deviations in parentheses, are given in Table 2.*

Table 2. *Final atomic parameters for DTPI*1 ($\times10^3$ *for* H *and* $\times10^4$ *for other atoms*)

For the non-hydrogen atoms, equivalent isotropic thermal parameters (*B*) were calculated from the refined anisotropic thermal parameters (Hamilton, 1959).

	x	*y*	*z*	*B* (Å^2)
S	2494·8 (5)	1250	1250	3·6
C(1)	1483 (2)	1250	1250	3·2
C(2)	1717 (2)	1468 (1)	1832 (14)	3·3
C(3)	2153 (2)	1495 (1)	1923 (13)	3·3
C(4)	2381 (2)	1725 (1)	2600 (13)	3·4
C(5)	2188 (2)	1946 (1)	1703 (16)	4·1
C(6)	2407 (2)	2161 (1)	2224 (19)	5·1
C(7)	2814 (2)	2163 (1)	3606 (19)	5·5
C(8)	3011 (2)	1948 (1)	4533 (17)	5·0
C(9)	2798 (2)	1730 (1)	3965 (16)	4·2
I(1)	3761 (2)	1298 (1)	−113 (12)	10·2
I(2)	1255 (3)	2323 (1)	4613 (15)	7·1
I(2*A*)	1250	2299 (2)	6250	4·8
I(3)	1265 (2)	2409 (2)	94 (13)	9·9
H(2)	157 (2)	160 (1)	244 (13)	4·2 (13)
H(5)	190 (2)	195 (1)	59 (14)	4·4 (12)
H(6)	229 (2)	230 (1)	161 (19)	7·7 (19)
H(7)	300 (2)	231 (1)	401 (15)	5·7 (14)
H(8)	329 (2)	194 (1)	579 (14)	4·7 (12)
H(9)	296 (1)	159 (1)	485 (12)	2·5 (10)

*DTPI*2

The structure determination of DTPI2 was concurrent with that of DTPI1 and followed a very similar path. Unit-cell data required the donor molecules also to have crystallographic 222 symmetry and to stack along *c*. In addition, the tetragonal symmetry dictated the orientation of the molecular axis. Again, the streaking of the precession photographs indicated that the iodine atoms formed one-dimensionally disordered chains of polyiodide ions along *c*. From the large number of streaks and their enhanced intensities, it was evident that there was a relatively high proportion of I atoms occupying the 9·7 Å incommensurate lattice of this form. The observed density of the crystals implied a unit-cell composition of two $\varphi_4\mathrm{DTP(I)}_{2\cdot25}$ units, which in $P\bar{4}b2$ corresponds to two symmetrically equivalent polyiodide chains per donor stack with approximately 0·56 I atoms per asymmetric unit. Resonance Raman spectra (Trotter, 1979) indicated only the presence of I_3^- ions.

An *hk*0 Patterson map yielded the *c*-axis projection of the entire structure. Subsequent three-dimensional electron density maps, initially phased with S and C(1), revealed the *z* parameters for the atoms of the donor molecule. A plausible model for the iodine chain allowed refinement of the donor molecule with anisotropic temperature factors, and the H atom positions were then obtained from a difference electron density map.

Complete refinement was again hampered by the disorder of the I atoms. Although the relatively intense streaking on the precession photographs indicated that a substantial portion of the I atoms occupied a lattice incommensurate with that of the donor, it was evident that the iodines also make substantial contributions to structure factors with $l \neq 0$. Also, the distribution of electron density along the channel, shown in Fig. 1(*c*), is not uniform along *c*. A single maximum is located on the twofold axis at $z = \frac{1}{2}$ with the electron density decreasing to about half the maximum value at $z = 0$. We attribute this distribution to the overlap of partially and unequally occupied, disordered atomic sites situated between the twofold axes, with the I atoms approximately *c*/4 apart, superimposed upon background density caused by the contribution of the incommensurate atoms to *hk*0 reflections.

The I_3^- model eventually adopted and refined consisted of I(1) atoms at approximately $z = \pm c/8$ and

---

* Lists of structure factors and anisotropic thermal parameters have been deposited with the British Library Lending Division as Supplementary Publication No. SUP 35169 (20 pp.). Copies may be obtained through The Executive Secretary, International Union of Crystallography, 5 Abbey Square, Chester CH1 2HU, England.

I(2) atoms at approximately $z = \frac{1}{2} \pm c/8$ with I(2)/I(1) occupancies in the ratio of 2/1. This model ideally requires an I_3^- ion to occupy three unit cells:

$$\mathrm{I}(2)\overset{3c/4}{\text{——}}\mathrm{I}(2)\overset{3c/4}{\text{——}}\mathrm{I}(1)\overset{6c/4}{\cdots\cdots}\mathrm{I}(2).$$

For 100% commensurate I atoms, the I(1) and I(2) occupancies would be 0·167 and 0·333, respectively, which results in a stoichiometry, φ_4DTP(I)$_{2\cdot00}$, deficient in iodine. For 100% incommensurability of the I atoms, the stoichiometry becomes φ_4DTP(I)$_{2\cdot30}$. Contributions by both lattices to a crystal results in intermediate compositions.

Refinement with isotropic thermal parameters for H and anisotropic thermal parameters for all other atoms, with occupancies of 0·193 for I(1) and 0·385 for I(2) to give a better stoichiometry, yielded $R = 0{\cdot}042$ ($R_w = 0{\cdot}050$) for a completely commensurate lattice. Included in the latter stages of the calculations was an extinction parameter (Larson, 1969), $g = 4{\cdot}1(1) \times 10^{-6}$, obtained by refining the 206 largest structure factors with unit weights. Although a good agreement factor was obtained, the refinement had not converged fully, since the β_{33} values for both I(1) and I(2) were increasing substantially with each refinement cycle.

The least-squares program was modified to include scattering contributions from 100% of the I atoms to $hk0$ reflections and from $(100 - N)$% of the I atoms to hkl, $l \neq 0$ reflections, where N is the percentage of I incommensurate with the subcell. Refinements were performed with $N = 50$, 60, 70 and 80% in which all parameters converged. Values of N less than 50% (except for $N = 0$ above) were not considered, since the stoichiometry was too iodine deficient for such compositions. The best agreement, $R = 0{\cdot}042$ ($R_w = 0{\cdot}054$), was obtained for $N = 50$, which corresponds to a stoichiometry φ_4DTP(I)$_{2\cdot15}$. We have taken this as our final refinement.

On the final cycle, all shifts were $<0{\cdot}1\sigma$. Residual density in a final difference electron density map was within $\pm0{\cdot}21$ e Å^{-3} except in the I channel where the residual density was generally negative with a maximum deviation of $-0{\cdot}81$ e Å^{-3}, indicating that the I atom contributions to the commensurate lattice were somewhat overestimated. The final atomic parameters with estimated standard deviations in parentheses are given in Table 3.* Figs. 2–4 described below were drawn with the aid of the computer program *ORTEP* II (Johnson, 1971).

Table 3. *Final atomic parameters for DTPI2* (× 10^3 *for* H *and* × 10^4 *for other atoms*)

For the non-hydrogen atoms, equivalent isotropic thermal parameters (B) were calculated from the refined anisotropic thermal parameters (Hamilton, 1959).

	x	y	z	B (Å^2)
S	3615·3 (5)	1384·7 (5)	0	3·3
C(1)	4742 (2)	258 (2)	0	3·1
C(2)	4914 (2)	949 (2)	575 (13)	3·0
C(3)	4469 (2)	1479 (2)	674 (12)	2·8
C(4)	4676 (2)	2190 (2)	1352 (12)	2·9
C(5)	5320 (2)	2418 (2)	449 (17)	3·7
C(6)	5507 (3)	3084 (3)	998 (15)	4·5
C(7)	5048 (3)	3536 (3)	2385 (15)	4·7
C(8)	4402 (3)	3323 (3)	3313 (15)	4·2
C(9)	4209 (3)	2650 (2)	2781 (14)	3·5
I(1)	7225 (5)	2277 (4)	1437 (31)	8·1
I(2)	7152 (4)	2163 (3)	3842 (15)	7·7
H(2)	536 (2)	107 (3)	114 (14)	4·5 (13)
H(5)	558 (3)	208 (3)	−85 (18)	5·5 (15)
H(6)	591 (4)	331 (3)	−24 (24)	7.8 (17)
H(7)	517 (3)	402 (3)	312 (13)	4·1 (11)
H(8)	410 (2)	363 (2)	433 (14)	3·6 (11)
H(9)	374 (2)	248 (2)	351 (11)	2·9 (9)

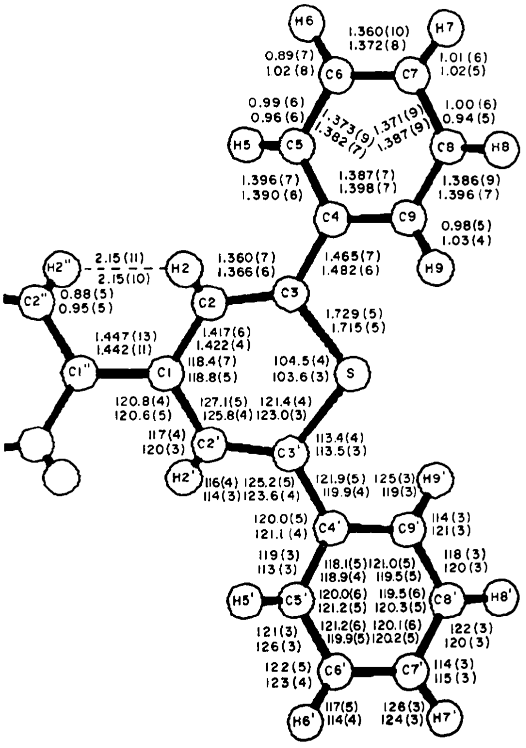

Fig. 2. Bond lengths (Å) and angles (°) for DTPI1 (upper figures) and DTPI2 (lower figures). Estimated standard deviations are given in parentheses.

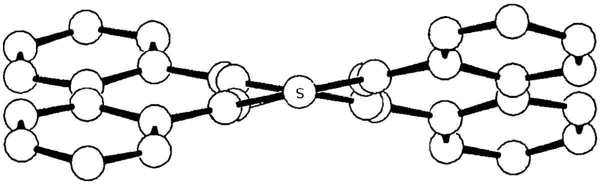

Fig. 3. DTPI1 viewed along the S···S vector.

---

* See previous footnote.

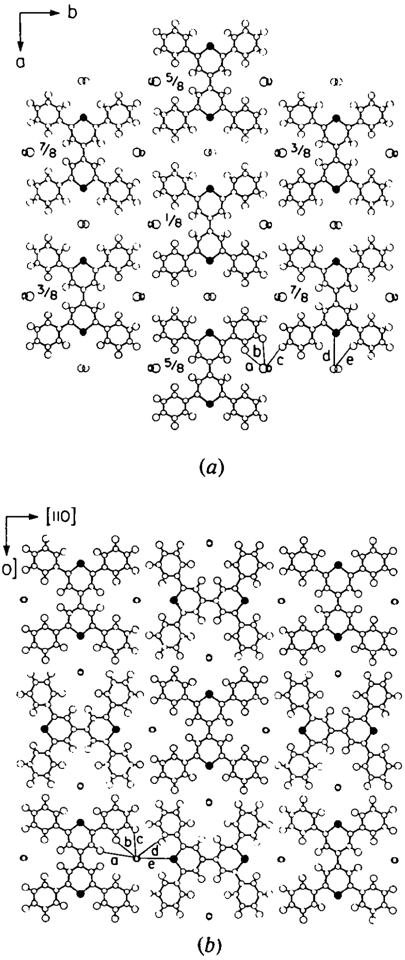

Fig. 4. (001) projections. (*a*) DTPI1. I(1) atoms occupy the channels between the S atoms. In the other I channels, the smaller atom is I(3) and the larger atom represents I(2) and I(2*A*). The fractions give the *z* coordinates of the centers of the DTP molecules. (*b*) DTPI2. I(1) is displaced toward S compared to I(2). All DTP molecules are centered at $z = 0$.

Discussion

The bond lengths and angles for the donor molecules in both structures are given in Fig. 2. There are no significant differences in the bond lengths of the two forms, the largest deviation being $2\cdot0\sigma$ for S—C(3). The angles, which are strongly influenced by packing forces, also agree well, the largest deviation being $3\cdot2\sigma$ for C(3)—C(4)—C(9). Because of the similarity in bond lengths, we believe that the donor molecules are partially oxidized to about the same degree in both DTPI1 and DTPI2. From the stoichiometry of the final refinements, $\varphi_4\mathrm{DTP}(\mathrm{I}_3)_{0\cdot36}(\mathrm{I}_5)_{0\cdot40}$ for DTPI1 and $\varphi_4\mathrm{DTP}(\mathrm{I}_3)_{0\cdot72}$ for DTPI2, one expects the donor radical cations to have formal net charges of $+0\cdot76$ for DTPI1 and $+0\cdot72$ for DTPI2, which are not very different. The alternative refinement for DTPI1, in which all I atoms were present as I_3^-, had a stoichiometry $\varphi_4\mathrm{DTP}(\mathrm{I}_3)_{1\cdot05}$, which implies a charge of at least $+1\cdot0$ for the donor ions and should give bond lengths for DTPI1 significantly different from those of DTPI2. This was one of the considerations that led us to the specific $\mathrm{I}_3^-/\mathrm{I}_5^-$ model used in the refinement of DTPI1.

The expected bond numbers (Pauling, 1960; Burke-Laing & Laing, 1976) for an average structure resulting from contributions of 26% neutral form (*a*) and 74% radical-ion form (*b*),

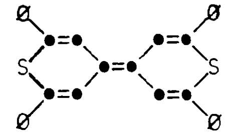

(*a*)

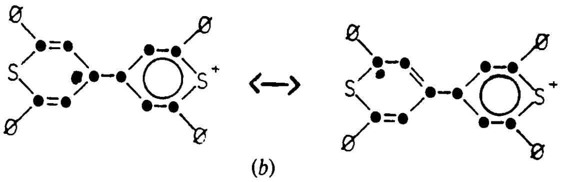

(*b*)

which has 12 approximately equivalent forms, are given in Table 4 along with a comparison of predicted bond lengths and the experimental values determined here. Agreement is fairly good, although the bridge bond [C(1)—C(1)″] is longer and C(1)—C(2) is shorter than predicted. The differences can be accounted for by postulating a form (*c*)

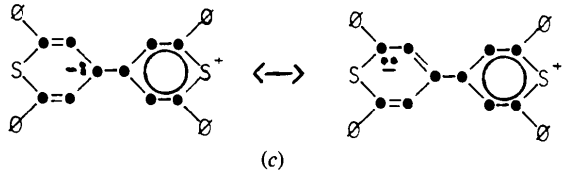

(*c*)

in which charges in the neutral molecule (*a*) have separated to form an aromatic sextet in one of the thiapyranylidene rings. Canonical structure (*c*) has 12 approximately equivalent forms which are completely analogous to the 12 forms of (*b*), and thus contributions from (*c*) produce the same effect as a larger formal positive charge. Predicted values of bond numbers and bond lengths for contributions of 74% (*b*), 20% (*a*), and 6% (*c*) are also given in Table 4. Predicted and experimental values show excellent agreement. The potential contribution of structures such as (*c*) is strongly supported by our structure determination for unoxidized φ_4DTP in which the bond lengths can be accounted for by a structure with 50% (*a*) and 50% (*c*) character (Luss & Smith, 1980).

Although the individual thiapyranylidene and phenyl rings are planar, the donor molecules are not, since the

Table 4. *Comparison of experimental bond lengths with expected values from bond-length bond-number curves*

Distances are in Å. Bond numbers are denoted by *n*, bond lengths by *r*.

	Predicted values 74% (*b*), 26% (*a*)		Experimental bond lengths		Predicted values 74% (*b*), 20% (*a*), 6% (*c*)	
	n	*r*	DTPI1	DTPI2	*r*	*n*
S–C(3)	1·19	*	1·729	1·715	*	1·20
C(1)–C(1)″	1·26	1·434	1·447	1·442	1·445	1·20
C(1)–C(2)	1·31	1·425	1·417	1·422	1·420	1·33
C(2)–C(3)	1·69	1·364	1·360	1·366	1·366	1·67
C(3)–C(4)	1·00	1·480	1·465	1·482	1·480	1·00

* A reliable estimate from bond-length bond-number curves is difficult. Various S–C_{sp^2} single-bond lengths have been proposed including 1·75 Å (Jones & Power, 1976), 1·77 Å (Argay, Kálmán, Nahlovski & Ribár, 1975), 1·82 Å (Abrahams, 1956) and 1·78 Å from the sum of the covalent radii (Pauling, 1960). The short S–C_{sp^2} bonds in this work indicate some degree of double-bond character and compare favorably with those found in TTT_2I_3 [av. – 1·738 (3) Å], where a bond number of 1·13 can be expected.

rings are all twisted relative to each other. This is evident from Fig. 3, in which the donor molecule is viewed along the S···S axis. The amount of twist is similar in both forms. The dihedral angles between the thiapyranylidene rings are 20·7° in DTPI1 and 20·9° in DTPI2. The thiapyranylidene and phenyl rings form dihedral angles of 26·1° in DTPI1 and 26·5° in DTPI2. The 21° angle between the thiapyranylidene rings is possible because of the high degree of single-bond character for C(1)–C(1)″. The twist, by reducing π overlap, may in turn enhance canonical form (*b*) at the expense of form (*a*), which also could account for the lengthening of C(1)–C(1)″ and the shortening of C(1)–C(2) compared to expected values.

The (001) projection of the DTPI1 structure is shown in Fig. 4(*a*). The positions of the centers of the φ_4DTP moieties are given to show that the molecules in cyclic groups of four donor stacks describe a helix; both right- and left-handed helices are present. The polyiodide ions fit into distinct channels between the stacks. The minimum distances (*a* through *e*, Fig. 4*a*) from H and S atoms to the midpoints of the I chains are: $a = 2{\cdot}99$, $b = 3{\cdot}24$, $c = 2{\cdot}97$, $d = 3{\cdot}89$, and $e = 3{\cdot}08$ Å. Except for *b*, these distances are all less than the sums of van der Waals radii [3·15 Å for I + H, 4·00 Å for I + S (Pauling, 1960)]. Thus, it appears that the channels are constricted by atoms of the donor subcell and the polyiodide ions are greatly inhibited from occupying the incommensurate lattice. Departures from linearity of the polyiodide ions are also caused by the constrictions of the channels. The measured contacts are as short as 3·06 (6) for I···H and 3·965 (8) Å for I(1)···S. Although the I···H distances would be even shorter if the 'true' positions of the H atoms were considered, the contacts are not unreasonable given the uncertainty in the I atom positions.

The bond lengths (Å) and angle in the I_3^- ions of DTPI1 are:

$$\mathrm{I(1)}\overset{2\cdot74\,(1)}{\text{———}}\underset{168\cdot9^\circ}{\mathrm{I(1)}}\overset{2\cdot86\,(1)}{\text{———}}\mathrm{I(1)}\overset{4\cdot54\,(1)}{\cdots\cdots}\mathrm{I(1)}.$$

The standard deviations given are from the least-squares process and do not reflect the uncertainties in iodine positions caused by the disorder. These bond distances compare to a normal value of about 2·92 Å, but the angle falls considerably outside the range 174–180° normally encountered (Runsink, Swen-Walstra & Migchelsen, 1972). The bond lengths (Å) and angles in the I_5^- ions are:

$$\mathrm{I(3)}\overset{2\cdot92\,(1)}{\text{———}}\underset{173\cdot0\,(4)^\circ}{\mathrm{I(2)}}\overset{3\cdot10\,(1)}{\text{———}}\underset{175\cdot1\,(6)^\circ}{\mathrm{I}(2A)}\overset{3\cdot10\,(1)}{\text{———}}\underset{173\cdot0\,(4)^\circ}{\mathrm{I(2)}}\overset{2\cdot92\,(1)}{\text{———}}\mathrm{I(3)}\overset{6\cdot55\,(1)}{\cdots\cdots}\mathrm{I(3)}.$$

These distances compare with the sequence 2·74, 3·26, 3·26, 2·74 and 3·50 Å reported for the analysis of diffuse layer lines in trimesic acid polyiodide (Herbstein & Kapon, 1972). Our non-bonded distance is large to allow the repeat of I_5^- ions of one type and one orientation. A shorter repeat distance could be realized if other configurations and orientations of I_5^- were allowed, but this would require the introduction of additional I atoms and would tend to equalize the electron densities along the columns, contrary to the observed distribution. Our model predicts a ratio of 3/2 for the electron densities around I(2) and I(3) and is consistent with values of the occupancies obtained in the least-squares refinement and with the low symmetry of the I(2)/I(3) channel.

The (001) projection of the DTPI2 structure is shown in Fig. 4(*b*). In this structure, the φ_4DTP ions lie in (001) sheets at the same *z* level so there is no helical arrangement as in DTPI1. As a result of the tetragonal symmetry, the molecular stacks pack with the side of one donor stack facing the end of the adjacent stack, and only one type of channel is formed which can accommodate polyiodide ions. The minimum distances from H and S atoms to the midpoint of the I_3^- chain ($a = 4{\cdot}27$, $b = 3{\cdot}22$, $c = 3{\cdot}36$, $d = 3{\cdot}10$, and $e = 3{\cdot}94$ Å, Fig. 4*b*) indicate that there is considerably less constriction here than in DTPI1. Hence, one might expect DTPI2 to exhibit a much greater degree of incommensurability than DTPI1. From the refinements the degree of incommensurability approaches 50% in DTPI2 but is very small in DTPI1. Observed short contacts are I(1)···S = 3·85 (1) and I(1)···H(9) = 3·12 (4) Å. These weak interactions help account for the confinement of approximately half of the I_3^- ions to the donor subcell as well as the 2/1 ratio for I(2)/I(1).

The bond lengths (Å) and angle of the I_3^- ions in DTPI2 are:

$$\mathrm{I(2)}\overset{2\cdot86\,(1)}{\text{———}}\underset{174\cdot7\,(5)^\circ}{\mathrm{I(2)}}\overset{2\cdot84\,(1)}{\text{———}}\mathrm{I(1)}\overset{5\cdot49\,(1)}{\cdots\cdots\cdots}\mathrm{I(2)}.$$

Both the angle and the bond distances are reasonable. The non-bonded distance is large and allows the repeat of I_3^- ions of one orientation. A shorter repeat distance requires the addition of I(1)–I(1)–I(2) units, which would tend to equalize the occupancies of I(1) and I(2) and would create more short I···S contacts. In addition, the I(1)–I(1) bond length, 2·66 Å, would be rather short. The 2/1 ratio of occupancies arising from I(2)–I(2)–I(1) triiodide ions is supported by the refinement, the electron density distribution, the short I(1)···S contact and the low symmetry of the channel.

The plane-to-plane separation of the thiapyranylidene rings is 3·64 in DTPI1 and 3·66 Å in DTPI2. The separation between planes through the phenyl rings is 3·42 in DTPI1 and 3·43 Å in DTPI2. These distances are all normal values and do not indicate any unusual interaction between donor molecules. All other intermolecular contacts were greater than the sums of van der Waals radii.

We thank Ms E. D. Schneider for providing the crystals, Dr J. H. Perlstein for suggesting the problem and for helpful discussions, and Dr P. J. Trotter for the resonance Raman results and for his convincing demonstration of the presence of I_5^- in DTPI1. We also thank Drs R. P. Scaringe and L. C. Isett for reading the manuscript and for discussions concerning the diffuse scattering. Dr Isett has pointed out to us that the extra streak at 2·7 Å for DTPI2 would actually equal 9·7 Å, the incommensurate I_3^- spacing, if measured from the $l = 1$ row of spots. This is consistent with scattering by a static charge density wave, a modulation on the φ_4DTP stack caused by the interaction of the incommensurate I_3^- chains with the conduction electrons on the φ_4DTP stack. From charge-neutrality considerations (Isett *et al.*, 1979*b*) the Fermi wave vector, $2k_F$, for this modulation is

$$2k_F = 2\pi f_D/2c = 2\pi/c' = 2\pi/9\cdot7,$$

where f_D is the fractional charge per donor which is 0·77 for a fully incommensurate triiodide component. It is possible that the modulation and the charge density wave could be associated with the commensurate I_3^- chains. We believe this is unlikely since it would require fractional charges for the triiodide ions. X-ray diffuse scattering experiments are needed to definitively explain the extra streak.

References

Abrahams, S. C. (1956). *Q. Rev. Chem. Soc.* **10**, 407–436.

Alizon, J., Blanc, J., Gallice, J., Robert, H., Fabre, C., Strzelecka, H., Rivory, J. & Weyl, C. (1977). *Lecture Notes in Physics*, 65, *Organic Conductors and Semiconductors*, edited by L. Pal, G. Gruner, A. Janossy & J. Solyom, pp. 563–569. New York: Springer.

Argay, Gy., Kálmán, A., Nahlovski, A. & Ribár, B. (1975). *Acta Cryst.* B**31**, 1956–1961.

Burke-Laing, M. & Laing, M. (1976). *Acta Cryst.* B**32**, 3216–3224.

Busing, W. R., Martin, K. O. & Levy, H. A. (1962). *ORFLS*. Report ORNL-TM-305. Oak Ridge National Laboratory, Tennessee.

Endres, H., Harms, R., Keller, H. J., Moroni, W., Nothe, D., Vartanian, M. H. & Soos, Z. G. (1979). *J. Phys. Chem. Solids*, **40**, 591–596.

Endres, H., Keller, H. J., Mégnamisi-Bélombé, M., Moroni, W., Pritzkow, H., Weiss, J. & Comès, R. (1976). *Acta Cryst.* A**32**, 954–957.

Hamilton, W. C. (1959). *Acta Cryst.* **12**, 609–610.

Herbstein, F. H. & Kapon, M. (1972). *Acta Cryst.* A**28**, S74–S75.

Huml, K. (1967). *Acta Cryst.* **22**, 29–32.

International Tables for X-ray Crystallography (1974). Vol. IV, chap. 2. Birmingham: Kynoch Press.

Isett, L. C. (1978). *Phys. Rev. B*, **18**, 439–447.

Isett, L. C. & Perez-Albuerne, E. A. (1977). *Solid State Commun.* **21**, 433–435.

Isett, L. C., Reynolds, G. A., Schneider, E. D. & Perlstein, J. H. (1979*a*). Unpublished results.

Isett, L. C., Reynolds, G. A., Schneider, E. D. & Perlstein, J. H. (1979*b*). *Solid State Commun.* **30**, 1–6.

Johnson, C. K. (1971). *ORTEP* II. Report ORNL-3794, second revision. Oak Ridge National Laboratory, Tennessee.

Jones, R. D. G. & Power, L. F. (1976). *Acta Cryst.* B**32**, 1801–1806.

Larson, A. C. (1969). *Crystallographic Computing*, edited by F. R. Ahmed, pp. 291–294. Copenhagen: Munksgaard.

Luss, H. R. & Smith, D. L. (1973). *Acta Cryst.* B**29**, 998–1005.

Luss, H. R. & Smith, D. L. (1980). *Acta Cryst.* B**36**, 986–989.

Pauling, L. (1960). *The Nature of the Chemical Bond*, 3rd ed. Ithaca: Cornell Univ. Press.

Perlstein, J. H. (1977). *Angew. Chem. Int. Ed. Engl.* **16**, 519–534.

Runsink, J., Swen-Walstra, S. & Migchelsen, T. (1972). *Acta Cryst.* B**28**, 1331–1335.

Smith, D. L. & Luss, H. R. (1977). *Acta Cryst.* B**33**, 1744–1749.

Stucky, G. D., Schultz, A. J. & Williams, J. M. (1977). *Annu. Rev. Mater. Sci.* **7**, 301–339.

Trotter, P. J. (1979). Unpublished results.